Flux pinning in Bi-2212/Ag-based wires and coils

P. Fabbricatore, C. Priano, A. Sciutti, G. Gemme, R. Musenich, and R. Parodi
Istituto Nazionale di Fisica Nucleare, Sezione di Genova, Via Dodecaneso 33, I 16146 Genova, Italy

F. Gömöry
Institute of Electrical Engineering, Slovak Academy of Sciences, Dubravska cesta, 84239 Bratislava, Slovak Republic

J. R. Thompson
Department of Physics, University of Tennessee, Knoxville, Tennessee 37996-1200
and Oak Ridge National Laboratory, Oak Ridge, Tennessee 37831-6061
(Received 1 May 1996)

This paper describes a study of pinning forces in Ag/Bi-based wires and small coils. The goal of this analysis is to characterize and to compare the main pinning mechanisms in wires (short samples) and prototype practical devices, e.g., coils (long samples). The effects of thermal activation were found to hinder the straightforward determination of the pinning parameters from the critical current data. However, we succeeded in extracting these parameters from the irreversibility line. The scaling law for the pinning force employing the irreversibility field in virtue of the scale for magnetic fields was derived theoretically. The best fit to the experimentally determined pinning forces gave the flux-creep model corresponding to the power-law current—voltage dependence $J \propto E^n$. [S0163-1829(96)01141-1]

I. INTRODUCTION

The objective of this work was to examine the current-carrying properties of some prototype superconducting devices and to characterize their vortex pinning properties via transport measurement of the critical current density and the irreversibility line (IL) $B_{\rm irr}=B_{\rm irr}(T_{\rm irr})$. This analysis is performed mostly in terms of the bulk pinning force density, $\mathbf{F_p}=\mathbf{J}_c(\mathbf{B},T)\times\mathbf{B}$ where B is the applied field and J_c is the critical current densities. It is generally accepted that the pinning force for conventional, hard type-II superconductors[1–5] can be well represented by the following factorized expression:

$$F_p = AB_{c2}^m b^\gamma (1-b)^\delta, \tag{1}$$

where A is a constant, B_{c2} is the upper critical field, $b=B/B_{c2}$ and m, γ, and δ are dimensionless factors whose values depend on the details of the pinning mechanism. The temperature dependence is included in $B_{c2}(T)$. As shown by Dew-Hughes,[6,7] the values of m and γ depend on defect geometry (pointlike, linear, planar or surface, etc.), type of interaction (core or magnetic) and type of pinning center (normal or superconductor having different properties with respect to the bulk). A comparison of the values of m, γ, δ for short samples versus coils, respectively, can give information about modifications of the pinning mechanism, if any, due to the different conditions during the winding and coil fabrication.

In the present work, we follow an approach similar to that of Matsushita,[8,9] in order to understand the main pinning mechanisms in wires and coils through the determination of the factors m and γ of Eq. (1). We can obtain information about these factors from critical current measurements as a function of field and temperature and complementary irreversibility line measurements.

Nevertheless, this kind of analysis is strongly affected by thermally activated flux creep, which modifies Eq. (1). In order to overcome this problem, we develop a simple model that includes flux creep, leading to a modified equation for the volume pinning force, which follows a scaling law as function of $B/B_{\rm irr}$.

II. CLASSICAL PINNING THEORIES

Fietz and Webb[1] introduced the idea of a factorized expression for the pinning force, with a form such as that in Eq. (1). Further work by Campbell and Evetts[2] and by Dew-Hughes[6] has shown that functions of the form of Eq. (1) can explain a variety of experimental results. The macroscopic pinning force can be considered as the result of the combined action of a large number of individual interactions, core or magnetic, between two ''lattices,'' the Abrikosov lattice of vortices and a generally disordered distribution of microstructural defects. Then one has[10]

$$F_p = \int_{-K_0}^{+K_0} K\rho(K)\,dK, \tag{2}$$

where $p(K)dK$ is the number of interactions per unit volume with forces between K and $K+dK$ and K_0 is the maximum force a pinning center of a given type can exert on a flux line.

Because of the strong coupling of flux lines to each other, their displacements due to the pinning interactions are generally small. Consequently, standard elastic theory can be used.[11] Furthermore, Brandt[12] has shown that linear elasticity theory has a very wide range of validity in high-T_c superconductors. As a specific illustration of Eq. (1), we have the expression

$$F_p \approx [B_{c2}^{9/2} b^{1/2}(1-b)/\kappa^3] \tag{3}$$

TABLE I. Scaling laws from early models of flux pinning: $F_p=[B_{c2}^m b^\gamma(1-b)^\delta/\kappa^\alpha]\Delta\kappa^\beta$.

Basic interaction, type of defects and interaction's distance	Pointlike defects lattice		Ref. No.	Superficial defects lattice		Ref. No.
Core interaction	$m=4.5$	$\gamma=0.5$		$m=1.5$	$\gamma=0.5$	
normal defect $L\ll\xi$	$\delta=1$	$\alpha=3$		$\delta=1$	$\alpha=2$	
ξ	$\beta=0$		11	$\beta=0$		6
Core interaction	$m=2.5$	$\gamma=0.5$		$m=2$	$\gamma=0.5$	
normal defect $L\gg\xi$	$\delta=1$	$\alpha=3$		$\delta=1$	$\alpha=2$	
ξ	$\beta=0$		3	$\beta=0$		6
Core interaction	$m=1.5$	$\gamma=0.5$		$m=1.5$	$\gamma=0.5$	
superconductive defect ($\Delta\kappa$)	$\delta=1$	$\alpha=5$		$\delta=1$	$\alpha=3$	
ξ	$\beta=2$		13	$\beta=2$		6
Core interaction	$m=2.5$	$\gamma=1.5$		$m=2$	$\gamma=1$	
superconductive defect ($\Delta\kappa$)	$\delta=1$	$\alpha=5$		$\delta=1$	$\alpha=3$	
a_0=Abrikosov lattice	$\beta=2$			$\beta=1$		
parameter			13			4
Magnetic	$m=2.5$	$\gamma=1.5$		$m=2$	$\gamma=0.5$	
λ	$\delta=1$	$\alpha=5$		$\delta=1$	$\alpha=3$	
	$\beta=0$		2	$\beta=0$		2

for a distribution of pointlike voids with dimension $L\ll\xi$, where ξ is the superconductive coherence length and $b=B/B_{c2}$ is the reduced field. This is a scaling law. Similar expressions are obtained for defects with different geometries, length scales, and types; several of these are collected in Table I. A central feature of these expressions for the pinning force is that they all have the general form of Eq. (1), but the exponents differ, depending on the geometrical and physical characteristics of the defect distribution. We can dismiss the magnetic pinning mechanism at the outset, however, as core pinning is stronger[14] by a factor of $\kappa/4\ln\kappa$. With $\kappa\geqslant 100$ in high-T_c superconductors, core pinning should dominate.

III. EFFECT OF CREEP

Classical pinning theory, some results of which are collected in Table I, does not include dynamic effects like thermally activated flux creep. As the effects of magnetic relaxation are relatively weak in most low-temperature superconductors, there was no specific need to incorporate such effects. In high-T_c superconductors, however, the transport and magnetic properties are strongly dependent on fluxon dynamics and these effects must be considered.[15] Yeshurun and Malozemoff explained successfully the form of the irreversibility line, by including large flux-creep effects in the critical-state model.[16] The pinning force one observe at the electrical field E is

$$F_p=BJ_c=BJ_{c0}\left[1-\frac{K_BT}{U_0}\ln\left(\frac{E_0}{E}\right)\right], \tag{4}$$

where J_{c0} is the critical current density without creep effects and E_0 is the minimum measurable electrical field. In this simple model, the activation energy U_0 is equivalent to the height of the barrier the flux line must overcome. Then it is proportional to the product of the volume density of the pinning force, the activation volume V, i.e., the volume of the flux line that can be coherently activated, and the distance the line must move. Much theoretical work was done to derive these quantities that differ for various types of pinning mechanisms and vary with respect to temperature, magnetic flux density, etc.[17] For the purpose of further calculations we suppose that

$$U_0=F_{p0}V\xi \tag{5}$$

with $F_{p0}=BJ_{c0}$ being the ''ideal'' pinning force without thermal activation and V as the activation volume, then one has from Eq. (4) the result that

$$F_p=F_{p0}-\frac{K_BT}{V\xi}\ln\left(\frac{E_0}{E}\right). \tag{6}$$

In this expression, we use for F_{p0} the scaling law given by Eq. (1), and assume that $B\ll B_{c2}$, which means that the factor $(1-b)$ is negligible. Let us considering two possibilities for the activation volume:[16] $V=d^3=(1.075)^3(\phi_0/B)^{3/2}$ or $V=d^2\xi=(1.075)^2(\phi_0/B)\xi$, where d is the flux-line spacing. Then we obtain the respective expressions:

$$F_p=C_1b^\gamma-C_2b^{3/2}, \tag{7}$$

where $C_1=AB_{c2}^m$ and

$$C_2=\frac{B_{c2}^{3/2}K_BT}{(1.075)^3\Phi_0^{3/2}\xi}\ln\left(\frac{E_0}{E}\right)$$

or

$$F_p=C_3b^\gamma-C_4b, \tag{8}$$

where $C_3=C_1=AB_{c2}^m$ and

$$C_4=\frac{B_{c2}K_BT}{(1.075)^2\Phi_0\xi^2}\ln\left(\frac{E_0}{E}\right).$$

In general, these are not scaling laws, because there is no clear separation into factors depending separately on T and on B. As we will see in a later paragraph, however, some conditions of creep allow us to put these expressions into the form of scaling laws with respect to a parameter which is not B_{c2}, but rather the irreversibility field B_{irr}.

We can obtain an expression for the irreversibility line by setting $F_p=0$ in Eqs. (7) and (8), using the following relations for the temperature dependences of the upper critical field and the coherence length:

$$B_{c2}(t)=B_{c2}(0)(1-t^2), \tag{9a}$$

$$\xi(t)=\xi_0(1-t)^{-1/2}, \tag{9b}$$

where $t=T/T_c$. Solving for the magnetic field, we have

$$B_{\mathrm{irr}}=K_1 t^{2/(2\gamma-3)}(1-t)^{1/(2\gamma-3)}(1-t^2)^{2(m-\gamma)/(2\gamma-3)} \tag{10}$$

with

$$K_1=\left[\frac{K_B T_c B_{c2}^{\gamma-m}(0)}{(1.075)^3 A\Phi_1^{3/2}\xi(0)}\ln\left(\frac{E_0}{E}\right)\right]^{2/(2\gamma-3)};$$

or

$$B_{\mathrm{irr}}=K_2 t^{1/(\gamma-1)}(1-t)^{1/(\gamma-1)}(1-t^2)^{(m-\gamma)/(1-\gamma)} \tag{11}$$

with

$$K_2=\left[\frac{K_B T_c B_{c2}^{\gamma-m}(0)}{(1.075)^2 A\Phi_0\xi^2(0)}\ln\left(\frac{E_0}{E}\right)\right]^{1/(\gamma-1)}$$

according to the two different definitions for the activation volume.

For T near T_c, one can obtain a simplified version[8] of Eqs. (10) and (11):

$$B_{\mathrm{irr}}\propto(1-t)^{\varepsilon}, \tag{12}$$

where $\varepsilon=2(m-\gamma)/(3-2\gamma)$ or $\varepsilon=(m-\gamma+1)/(1-\gamma)$, depending on the activation volume.

The approach leading to the irreversibility field, as given in Eqs. (10) or (11), is based on Eq. (4), which is strictly valid only for current close to the critical current. A more general approach would take into account the measured E-J characteristics, which can be expressed by the following formula:[18]

$$J=J_0\left(\frac{E}{E_0}\right)^{K_B T/U_0}, \tag{13}$$

where E_0 and J_0 form a point on the characteristic E-J curve taken at an electric field E as low as possible.

Using Eq. (13) it is possible to write the volume pinning force as

$$F_p=BJ_c=BJ_0\left(\frac{E_c}{E_0}\right)^{K_B T/F_{p0}V\xi}, \tag{14}$$

where E_c is the field criterion used to define J_c. We use the criterion $E_c=0.1$ μV/cm for the experiments presented in this paper.

To define the irreversibility line, let us introduce a current threshold criterion J_{irr}, say 10^5 A/m^2=10 A/cm^2, above which the pinning force is negligibly small. Then putting $J=J_{\mathrm{irr}}$ and $B=B_{\mathrm{irr}}$ in Eq. (13) we can obtain another expression for the irreversibility line. Thus we find

$$B_{\mathrm{irr}}=K_3 t^{2/(2\gamma-3)}(1-t)^{1/(2\gamma-3)}(1-t^2)^{2(m-\gamma)/(2\gamma-3)} \tag{15}$$

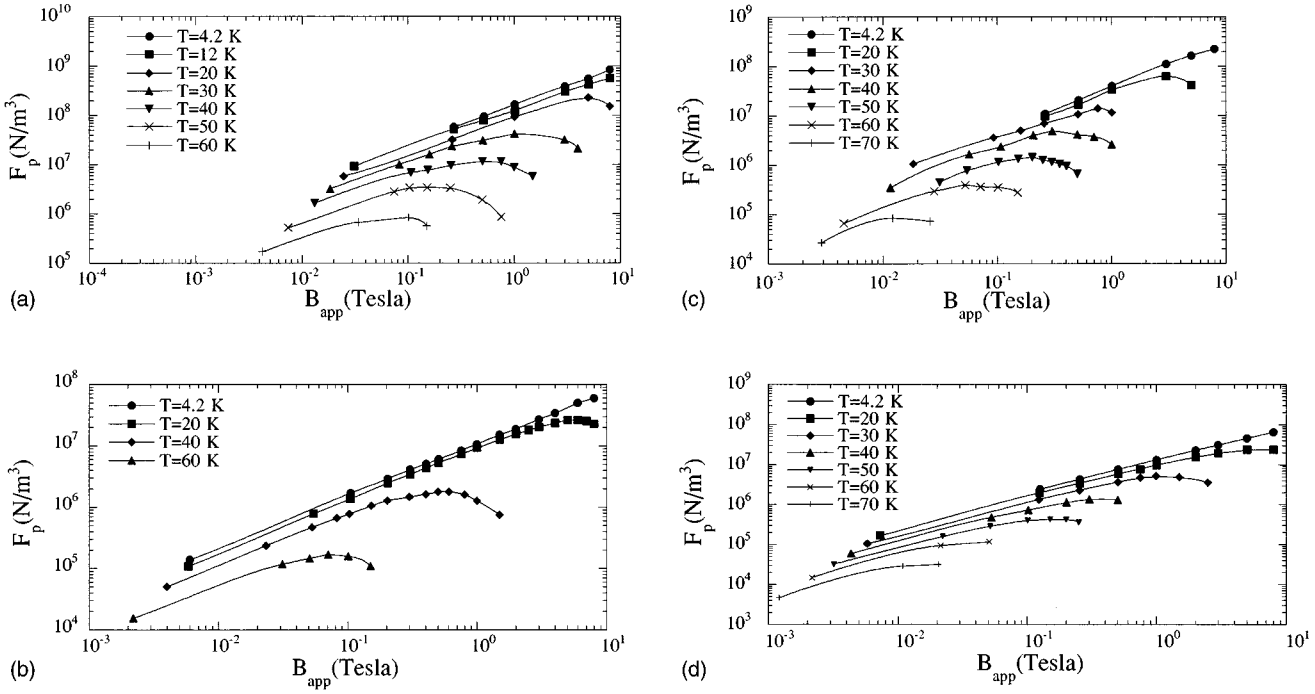

FIG. 1. Pinning force behavior vs magnetic field at different temperatures for the four samples of Bi-2212/Ag superconducting materials: (a) S-Vac, (b) C-Vac, (c) S-Pi, (d) C-Pi.

TABLE II. Measured pinning parameters found using Eqs. (1) and (10), (15) or Eqs. (11) and (16).

	γ			m		
Samples	From F_p Eq. (1)	From Eqs. (10)–(15)	IL Eqs. (11)–(16)	From F_p Eq. (1)	From Eqs. (10)–(15)	IL Eqs. (11)–(16)
S-Pi	0.93±0.09	0.5±0.3	0.8±0.3	4.7±0.5	2.2±0.5	2.2±0.5
S-Vac	0.81±0.09	0.5±0.3	0.8±0.2	3.5±0.7	2.3±0.6	2.3±0.6
C-Pi	0.81±0.08	0.8±0.3	0.7±0.3	5.0±0.9	2.6±0.4	2.6±0.4
C-Vac	0.89±0.09	0.8±0.3	0.7±0.4	3.4±0.8	2.4±0.5	2.4±0.5

with

$$K_3=\left(\frac{K_B T_c \ln E_c/E_0 B_{c2}(0)^{\gamma-m}}{\ln J_{\rm irr}/J_0 A(1.075)^3\Phi_0^{3/2}\xi(0)}\right)^{2/(\gamma-3)} \quad \text{for } V=d^3$$

and

$$B_{\rm irr}=K_4 t^{1/(\gamma-1)}(1-t)1/(\gamma-1)(1-t^2)^{(\gamma-m)/(\gamma-1)} \tag{16}$$

with

$$K_4=\left(\frac{K_B T_c \ln E_c/E_0 B_{c2}(0)^{\gamma-m}}{\ln J_{\rm irr}/J_0 A(1.075)^2\Phi_0\xi(0)^2}\right)^{1/(\gamma-1)} \quad \text{for} \quad V=d^2\xi.$$

Let us note that these temperature dependences of the irreversibility line are exactly the same as those obtained using for the creep the Anderson's model Eq. (4). The only difference between the two approaches is the expression of the constant K_i.

We see that the irreversible behavior of a high-T_c superconductor is related to the characteristics of the pinning force. In this analysis the irreversibility line is a function of m and γ, which are characteristic of the pinning mechanism inside the material. Thus both critical current and IL measurements can give information about the pinning mechanisms, in this analysis.

IV. EXPERIMENTAL DETERMINATION OF PINNING PARAMETERS

The samples analyzed in this paper were two Bi-2212/Ag sheathed round wires, produced by Pirelli and Vacuumschmelze (denoted as *S*-Pi and *S*-Vac) and two small coils wound using the Pirelli wire (*C*-Pi) and the Vacuumschmelze wire (*C*-Vac).

The wires *S*-Pi and *S*-Vac, of diameter 1 mm, are composed of a multicore superconductor (19 cores, $\phi_{\rm core}\approx 100$ μm), enclosed in a silver sheath. The test coils *C*-Pi, of internal diameter 30 mm and 50 mm height, and *C*-Vac of internal diameter 15 mm and 50 mm height were made with the wind-and-react technique. They were wound using wire of 4 and 10 m length, respectively, on a removable mandrel to avoid degradation of the transport properties due to the mechanical coupling with supporting structures.[19] The short sample and the test coil were thermally reacted in the-same way and at the same time. In order to melt the precursor of the Bi-2212 phase, the samples were heated up to 910 °C for 1 h; the crystallization was carried out at 840 °C for 100 h.

As we suggested before it is possible to extract information about pinning mechanism (m, γ factors) in two different ways:[8] from critical current measurements and from irreversibility line measurements.

The critical current measurements are carried out at different magnetic fields and temperatures. The critical current density is defined by the electric-field criterion of $E_c=0.1$ μV/cm and was obtained from *I*-*V* measurements, with the

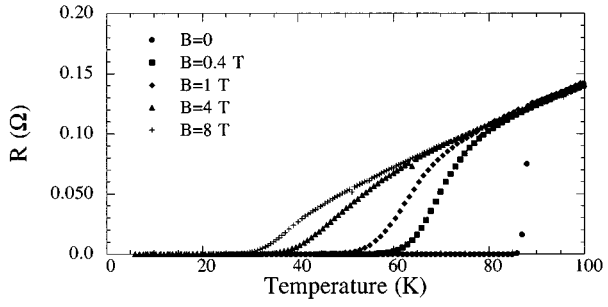

FIG. 2. Resistive measurements for the sample *C*-Vac at different applied magnetic fields.

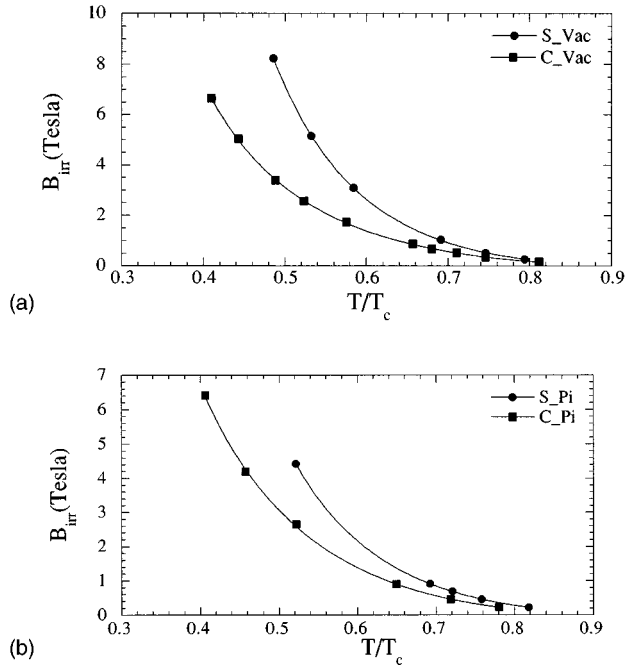

FIG. 3. Temperature dependence of the irreversibility field carried out from resistive measurements; (a) *S*-Vac and *C*-Vac; (b) *S*-Pi and *C*-Pi. Solid lines are the fit with Eq. (15).

parallel conduction of the Ag cladding subtracted out always.

The samples were field cooled. After each critical current measurement vs field at fixed temperature, the samples were heated above the critical temperature T_c to release trapped flux. The pinning forces measurements at different fields and temperature for the four samples are shown in Fig. 1.

Though the pinning force is strongly affected by dynamical effects, we can extract information about the pinning mechanisms by looking first at the part of the curves at low temperatures and low field; i.e., the portion less influenced by flux creep. Consequently, we consider selected data from the initial rising part of the $F_p(B)$ curves for each temperature. Using Eq. (1) for $B \ll B_{c2}$ the pinning force is approximated:

$$F_p \propto B_{c2}^m b^\gamma \propto B_{c2}(0)^{m-\gamma}(1-t^2)^{m-\gamma}B^\gamma. \tag{17}$$

The values of γ and m are found from a fit of the selected experimental data. From Eq. (17), the curves of F_p can be approximated at a fixed temperature as $F_p \propto B^\gamma$, so doing we found γ. Similarly we can evaluate $(m-\gamma)$ approximating the curves of F_p at a fixed field as $F_p \propto (1-t^2)^{m-\gamma}$.

In order to minimize the effect of flux creep, we use for γ a value found by extrapolating to $T=0$ the values determined at higher temperatures. In the same way, the values of $(m\text{-}\gamma)$ are found by extrapolating to $B=0$ the values determined at higher fields. The results for γ and m are shown in Table II.

A different approach, leading to the determination of the pinning parameters, is based on the measurements of the irreversibility field as function of temperature. Using Eqs. (10) and (11) or (15) and (16), respectively, we can fit the experimental data and obtain γ and m.

The irreversibility line is obtained from resistive transition measurements (e.g., see Fig. 2 for C-Vac) made at fixed field using the criterion $J_{\rm irr}=105$ A/m^2. At a fixed field B^* we define as T^* the temperature at which the electrical field across the sample is exactly $E_c=0.1$ μV/cm. Plotting the current density in the superconducting cross section $J_{\rm sc}$ versus T we find $J_{\rm sc}^*=J_{\rm sc}(T^*)$ so that we obtain one point of the curves $J_c(B)_{T=T}^*$ that follow the form:[20]

$$J_c(B)=J_0 e^{-a(T)B}. \tag{18}$$

From critical current measurements it is possible to obtain a formula for $a(T)$, so that evaluating $a(T^*)$ we can find $B_{\rm irr}$ from the following system:

$$\begin{aligned} J^* &= J_0 e^{-a(T^*)B^*}, \\ J_{\rm irr} &= J_0 e^{-a(T^*)B_{\rm irr}}, \end{aligned} \tag{19}$$

solving for $B_{\rm irr}$ we obtain

$$B_{\rm irr}=B^*+\frac{1}{a(T^*)}\ln\left(\frac{J^*}{J_{\rm irr}}\right). \tag{20}$$

In Fig. 3 is shown the behavior of the irreversible magnetic field vs temperature for our samples.

Analysis of the irreversibility line data, acquired mostly at higher temperatures, leads the values $\gamma \approx 0.5$–0.8 and $m \approx 2.5$, independent of which activation volume is assumed. Referring to the theoretical results in Table I, we see that the

TABLE III. Values of experimental pinning parameters found using Eq. (21), $F_p \propto (B/B_{\rm irr})$.

Samples	p	q
S-Pi	0.84±0.07	3.9±0.4
S-Vac	0.81±0.06	5.1±0.1
C-Pi	0.87±0.02	3.0±0.1
C-Vac	0.82±0.02	2.6±0.1

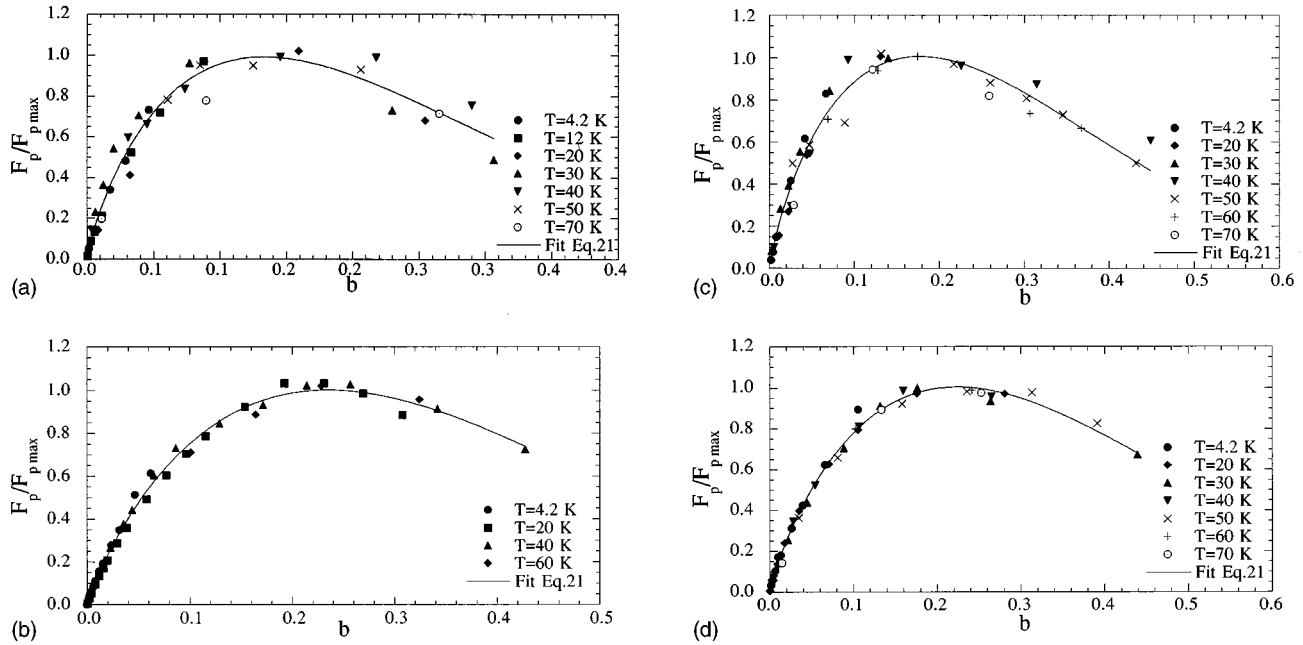

FIG. 4. Fit of the normalized pinning force ($F_p/F_{p\ \rm max}$) versus the normalized magnetic field ($B/B_{\rm irr}$) with the empirical Eq. (21). (a) S-Vac, (b) C-Vac, (c) S-Pi, (d) C-Pi.

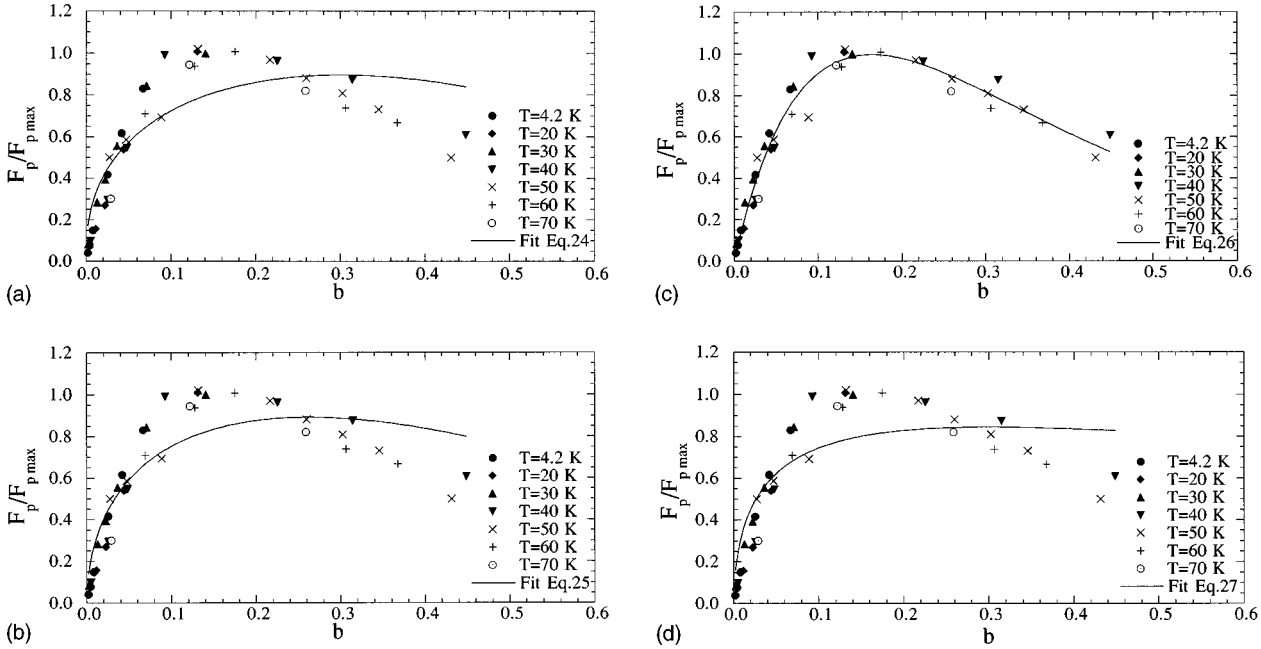

FIG. 5. Fit of the normalized pinning force ($F_p/F_{p\ \max}$) of short wire *S*-Pi versus the normalized magnetic field ($B/B_{\rm irr}$): (a) fitted with Eq. (24), (b) fitted with Eq. (25), (c) fitted with Eq. (26), (d) fitted with Eq. (27).

experimental values are consistent with core pinning by normal state, equiaxed defects with $L \gg \xi$, such as second phase inclusions, etc. On the other hand, the preliminary analysis of F_p using Eq. (1) gave the values $\gamma \approx 0.8$–0.9 and $m \approx 3.5$–5. While these latter values show no clear agreement with the mechanisms in Table I, the value of m is compatible with core pinning by normal pointlike defects with $L \ll \xi$. Oxygen vacancies, site-antisite defects and interstitials, which are generally present in cuprate superconductors, may all serve as pointlike pinning sites. For example, earlier flux-creep studies of pinning in $YBa_2Cu_3O_{7-\delta}$ crystals, under conditions where pointlike defects should be dominant, showed good agreement with theoretically predicted behavior for such a system.[21]

We think that this discrepancy between the two cases is due to the high influence of dynamic effects, which are especially pronounced at elevated temperatures. A partial introduction of creep effects through the evaluation of the irreversibility field, $B_{\rm irr}$, gives results more consistent with the values of Table I. This consideration leads us to try to understand better the temperature dependence of F_p, studying how Eq. (1) is modified by flux creep.

V. PINNING, CREEP, AND THE IRREVERSIBILITY LINE

Taking into account creep effects we cannot avoid considering the existence of a scaling law for high-T_c superconductors, which has been observed by several authors.[22–26] The observed pinning force can be expressed by the empirical law:

$$F_p \propto \left(\frac{B}{B_{\rm irr}}\right)^p \left(1-\frac{B}{B_{\rm irr}}\right)^q . \tag{21}$$

Here, the scaling field is the irreversibility field $B_{\rm irr}$ rather than the factor B_{c2} that appears in Eq. (1) for conventional superconductors. Equation (21) describes our experimental results very well, as evident in Fig. 4 showing fits to the normalized F_p data. The resulting values for p and q, which are given in Table III, are not far from those determined in other laboratories.[26] Note that the factor p is equivalent to γ and our value of $p \approx 0.8$ is similar to the value of γ found in the IL analysis.

A less empirical approach can be tried using expressions (7) and (8) or (14) for the pinning force. In fact expressions (7) and (8) obtained in the third paragraph are not scaling laws with respect to B_{c2} (the temperature dependence is not factorable), but they can be cast into the form of scaling laws with respect to $B_{\rm irr}$.

We can find an expression for B_{c2} as function of $B_{\rm irr}$ from Eqs. (7) and (8) by setting $F_p = 0$ and $B = B_{\rm irr}$:

$$B_{c2} = \left(\frac{K_B T}{A(1.075)^3 \Phi_0^{3/2} \xi \ln\dfrac{E_0}{E}}\right)^{1/(m-y)} B_{\rm irr}^{(3-2\gamma)/2(m-\gamma)} \tag{22}$$

for $V = d^3$ and

$$B_{c2} = \left(\frac{K_B T}{A(1.075)^2 \Phi_0 \xi^2 \ln\dfrac{E_0}{E}}\right)^{1/(m-y)} B_{\rm irr}^{(1-\gamma)/(m-\gamma)} \tag{23}$$

TABLE IV. Comparison of the exponent of Eqs. (15) and (26).

Samples	γ Eq. (26)	γ Eq. (15)
S-Pi	0.6±0.1	0.5±0.3
S-Vac	0.6±0.1	0.5±0.3
C-Pi	0.5±0.1	0.8±0.3
C-Vac	0.5±0.1	0.8±0.3

for $V=d^2\xi$.

Inserting Eqs. (22) and (23) in Eq. (4) we have for $V=d^3$,

$$F_p=R_1 b^{\gamma}(1-b^{3/2-\gamma}) \tag{24}$$

with

$$b=\frac{B}{B_{\rm irr}} \quad \text{and} \quad R_1=\frac{K_B T \ln E_0/E}{(1.075)^3\Phi_0^{3/2}\xi}B_{\rm irr}^{3/2}$$

and for $V=d^2\xi$,

$$F_p=R_2 b^{\gamma}(1-b^{1-\gamma}) \tag{25}$$

with

$$b=\frac{B}{B_{\rm irr}} \quad \text{and} \quad R_2=\frac{K_B T \ln E_0/E}{(1.075)^2\Phi_0\xi^2}B_{\rm irr}.$$

The temperature dependence is contained in the factors R_1 and R_2. The two dependences, from temperature and magnetic field, are factorized and the scaling field is exactly $B_{\rm irr}$. Thus we obtain a scaling law similar to the empirical one, but better justified.

In the same way we can obtain a scaling law starting from Eq. (14) and so doing we found:

$$F_p=R_3 b C^{b^{3/2\gamma}} \tag{26}$$

with $R_3=J_0 B_{\rm irr}$ and $C=(E_c/E_0)^{\ln(J_{\rm irr}/J_0)/\ln(E_c/E_0)}$ for $V=d^3$ and

$$F_p=R_3 b C^{b^{1-\gamma}} \tag{27}$$

for $V=d^2\xi$. We stress again that our formulas are carried out in the approximation $B \ll B_{c2}$.

Equations (24), (25), (26), and (27) give direct information only on γ, in fact the information on m is completely included in $B_{\rm irr}$. Also the information on γ obtained using the scaling laws is more significant in principle than that obtained from the IL, since we use all of the $F_p(b)$ data, rather than just one point that determines the irreversibility field. Let us now test the ability of the various relations to describe the set of measurements on the short Pirelli wire *S*-Pi. The results are shown in Fig. 5, where the discrete points are the experimental values. The four lines show the best fits to Eqs. (24)–(27), as indicated in the figure legend. It is readily apparent that the fit is quite poor in three cases. In contrast, Eq. (26), which is derived from the E-J relation for the $V=d^3$ case, describes the experimental measurements fairly well. This last analysis yields for γ the value 0.6, as listed in Table IV.

With this encouraging result, let us see how well the same model relation Eq. (26) describes $F_p(b)$ for the short sample of Vacuumschmelze wire (*S*-Vac) and the two small coils, wound and reacted from these materials. The results are shown in Figs. 6(a)–6(c). Examination of the figures shows a fairly good description for these three additional cases. The resulting values of γ, tabulated in Table IV, all fall in the range 0.5–0.6. As evident in Table IV, these results are very comparable with those from the IL analysis [Eq. (15)], where we obtained $\gamma=0.5$–0.8. These two set of results (based on the IL and on F_p with flux creep included) have much better

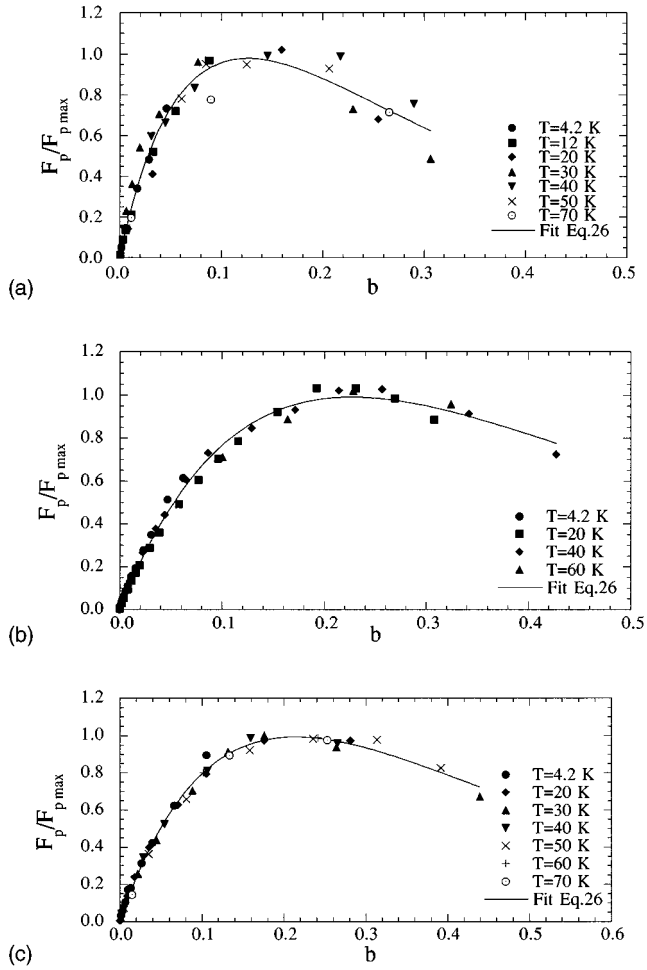

FIG. 6. Fit of the normalized pinning force ($F_p/F_{p\ \max}$) versus the normalized magnetic field ($B/B_{\rm irr}$) with Eq. (26), for materials. (a) *S*-Vac, (b) *C*-Vac, (c) *C*-Pi.

internal consistency, compared with the analysis based on conventional theory [Eq. (1)], where $\gamma=0.8$–0.9.

For the most part, this work treats vortex pinning from an aggregate, macroscopic perspective. It is clear, however, that these are very complex superconducting materials. The layered Bi-2212 itself is highly anisotropic, with idealized single-crystal experiments revealing markedly different properties for in-plane versus c-axis orientations of current and magnetic field. Correspondingly, a sophisticated theory has been developed to treat some aspects of this many faceted problem.[27] By contrast, the ''real'' materials (round wires and coils fabricated from them) investigated in this study have a wide distribution of angles between the current, magnetic field, and copper-oxygen planes. Qualitatively, one expects (1) that the bulk of the current flows in the CuO planes and (2) the current-limiting orientation of field occurs for H perpendicular to the planes (with H parallel to the CuO planes, intrinsic pinning is strong and robust).

Still, this leaves current flow through a percolative network of strongly coupled grain boundaries,[28–30] with currents in twisted and tortuous configurations. The pronounced, multiple, and interacting complexity of these effects makes some macroscopic, ''average'' treatment highly desirable. Hence we have tested the limits of the applicability of classical expressions for the pinning force density and found, not

surprisingly, that inclusion of flux-creep effects is essential. Together, the formalism provides a reasonably good ''big picture'' description of these complex materials, which can facilitate studies like the present intercomparison of short section wire and prototype small coils.

VI. CONCLUSIONS

We have studied the parameters of flux pinning in Bi-2212 short and long samples, analyzing the critical current density and irreversibility line determined experimentally. The pinning force under conditions of strong flux creep was derived for the cases when the activation volume V is proportional to d^3 and d^2, respectively, supposing the activation energy $U_0 \sim V$. We showed that for two models describing the flux-creep portion of the current-voltage characteristics, the Kim-Anderson model $J \sim \ln(E)$ and the power-law model $J \sim E^{K_B t/U_0}$, the calculated irreversibility lines have temperature dependences containing the pinning parameters. This result allowed us to use the irreversibility line data as an alternative source of information about the flux pinning in studied samples.

We have demonstrated that for supposed model cases ($U_0 \sim V$ with $V \sim d^3$ or $V \sim d^2$,) it is possible to find an analytical relation between B_{c2} and $B_{\rm irr}$. This leads to a scaling law for the pinning force where the irreversibility field $B_{\rm irr}$ serves as the scale for magnetic fields as often observed.

The main conclusions about the pinning in Bi-2212 short and long samples, in the range of fields and temperatures that we have considered are these:

(1) Both short and long samples seem dominated by mechanisms with vortex core pinning by normal, equiaxed defects. A conventional analysis of F_p, which tends to emphasise the lower temperature regime, suggest pinning by pointlike defects with dimension $L \ll \xi$, such as oxygen vacancies, site-antisite defects, and interstitials. Analysis of the irreversibility line, which emphasizes the regime of higher temperatures, suggests pinning by larger defects with $L \gg \xi$, e.g., precipitates.

(2) The same mechanisms operate in the short samples and in the small coils, even though the fabrication process caused a degradation of the transport properties (lower current densities and lower irreversibility line).

(3) A scaling law of F_p versus $B/B_{\rm irr}$ exists and can be obtained from the power-law E-J relationship.

(4) The system appears to have a $V = d^3$ dependence for the activation volume.

(5) The information on the pinning mechanism obtained from J_c measurements by selecting some data, to avoid creep effects, does not give consistent information, in fact the factors $\gamma \approx 0.8$–0.9 and $m \approx 4$ disagree with any mechanism of Table I.

[1] W. A. Fietz and W. W. Webb, Phys. Rev. **178**, 657 (1969).
[2] A. M. Campbell and J. E. Evetts, Adv. Phys. **21**, 199 (1972).
[3] G. Antesberger and H. Ullmaier, Philos. Mag. **29**, 1101 (1974).
[4] R. G. Hampshire and M. T. Taylor, J. Phys. F **2**, 89 (1972).
[5] R. I. Coote, R. I. Evetts, and A. M. Campbell, Can. J. Phys. **50**, 421 (1972).
[6] D. Dew-Hughes, Philos. Mag. **30**, 293 (1974).
[7] D. Dew-Hughes, Philos. Mag. B **55**, 459 (1987).
[8] T. Matsushita, E. S. Otabe, M. Kiuchi, B. Ni, T. Hikata, and K. Sato, Physica C **201**, 151 (1992).
[9] T. Matsushita, T. Fujiyoshi, K. Toko, and K. Yamafuji, Appl. Phys. Lett. **56**, 2039 (1990).
[10] H. Ullmaier, in *Irreversible Properties of Type-II Superconductors* (Springer-Verlag, Berlin, 1975).
[11] H. C. Freyhardt, Philos. Mag. **23**, 369 (1971).
[12] E. H. Brandt, Phys. Rev. Lett. **69**, 1105 (1992).
[13] R. Labush, Cryst. Lattice Defects **1**, 1 (1969).
[14] R. P. Huebener, *Magnetic Flux Structures in Superconductors* (Springer-Verlag, Berlin, 1979).
[15] A. P. Malozemoff and P. H. Kes, Phys. Rev. B **38**, 7203 (1988).
[16] Y. Yeshurun and A. P. Malozemoff, Phys. Rev. Lett. **60**, 2202 (1988).
[17] G. Blatter, M. V. Feigel'man, V. B. Geshkenbein, A. I. Larkin, and M. V. Vinokur, Rev. Mod. Phys. **66**, 1125 (1994).
[18] J. Z. Sun, C. B. Eom, B. Lairson, J. C. Bravan, and T. H. Geballe, Phys. Rev. B **43**, 3002 (1991).
[19] M. Ariante *et al.*, Cryogenics **34**, 809 (1994).
[20] P. W. Anderson, Phys. Rev. Lett. **8**, 250 (1962).
[21] J. R. Thompson, Y. R. Sun, D. K. Christen, L. Civale, A. D. Marwick, and F. Holtzberg, Phys. Rev. B **49**, 13 287 (1994).
[22] K. Kishio *et al.*, Supercond. Sci. Technol. **5**, S69 (1992).
[23] R. Wördenweber, K. Heinemann, G. V. S. Sastry, and H. C. Freyhardt, Cryogenics **29**, 458 (1990).
[24] R. A. Rose, S. B. Ota, P. A. J. de Groot, and B. Jayaram, Physica C **170**, 51 (1990).
[25] L. Neil, Cryogenics **32**, 975 (1992).
[26] L. Civale, M. W. McElfresh, A. D. Marwick, F. Holtzberg, C. Feild, J. R. Thompson, and D. K. Christen, Phys. Rev. B **43**, 13 732 (1991).
[27] G. Blatter, M. V. Feigel'man, V. B. Geshkenbein, A. I. Larkin, and V. M. Vinokur, Rev. Mod. Phys. **66**, 1125 (1994).
[28] A. Goyal *et al.*, Appl. Phys. Lett. **66**, 2903 (1995).
[29] A. E. Pashitski, A. Polyanskii, A. Gurevich, J. A. Parrell, and D. C. Larbalestier, Physica C **246**, 133 (1995).
[30] E. D. Specht, A. Goyal, and D. M. Kroeger, Phys. Rev. B **53**, 3585 (1996).